European Journal of Neuroscience, Vol. 27, pp. 1647–1658, 2008 doi:10.1111/j.1460-9568.2008.06136.x

Differential synaptic plasticity of the corticostriatal and thalamostriatal systems in an MPTP-treated monkey model of parkinsonism

Dinesh V. Raju,[1] Todd H. Ahern,[1] Deep J. Shah,[2] Terrence M. Wright,[3] David G. Standaert,[4] Randy A. Hall[5] and Yoland Smith[1,6]
[1]Yerkes National Primate Research Center,
[2]University of Georgia, Athens, GA 30609, USA
[3]Departments of Biology,
[5]Pharmacology and [6]Neurology, Emory University, Atlanta, GA 30322, USA
[4]Department of Neurology, University of Alabama at Birmingham, Birmingham, AL 35294, USA

Keywords: non-human primate, striatum, ultrastructure, vGluT1, vGluT2

Abstract

Two cardinal features of Parkinson's disease (PD) pathophysiology are a loss of glutamatergic synapses paradoxically accompanied by an increased glutamatergic transmission to the striatum. The exact substrate of this increased glutamatergic drive remains unclear. The striatum receives glutamatergic inputs from the thalamus and the cerebral cortex. Using vesicular glutamate transporters (vGluTs) 1 and 2 as markers of the corticostriatal and thalamostriatal afferents, respectively, we examined changes in the synaptology and relative prevalence of striatal glutamatergic inputs in methyl-4-phenyl-1,2,3,6-tetrahydropyridine (MPTP)-treated monkeys using electron microscopic immunoperoxidase and confocal immunofluorescence methods. Our findings demonstrate that the prevalence of vGluT1-containing terminals is significantly increased in the striatum of MPTP-treated monkeys (51.9 ± 3.5% to 66.5 ± 3.4% total glutamatergic boutons), without any significant change in the pattern of synaptic connectivity; more than 95% of vGluT1-immunolabeled terminals formed axo-spinous synapses in both conditions. In contrast, the prevalence of vGluT2-immunoreactive terminals did not change after MPTP treatment (21.7 ± 1.3% vs. 21.6 ± 1.2% total glutamatergic boutons). However, a substantial increase in the ratio of axo-spinous to axo-dendritic synapses formed by vGluT2-immunoreactive terminals was found in the pre-caudate and post-putamen striatal regions of MPTP-treated monkeys, suggesting a certain degree of synaptic reorganization of the thalamostriatal system in parkinsonism. About 20% of putative glutamatergic terminals did not show immunoreactivity in striatal tissue immunostained for both vGluT1 and vGluT2, suggesting the expression of another vGluT in these boutons. These findings provide striking evidence that suggests a differential degree of plasticity of the corticostriatal and thalamostriatal system in PD.

Introduction

Nigrostriatal dopamine depletion disrupts the functional interplay between dopamine and glutamate in Parkinson's disease (PD) (Graybiel, 1990; Kotter, 1994; Starr, 1995; Calabresi *et al*., 1997). The loss of dopamine is associated with increased diameter of postsynaptic densities at corticostriatal synapses of 6-hydroxydopamine (6-OHDA)-treated rats (Ingham *et al*., 1993) and PD patients (Anglade *et al*., 1996), suggesting hyperactivity at these glutamatergic synapses. These findings are consistent with rodent data showing that unilateral dopamine depletion leads to increased intrastriatal glutamate levels (Lindefors & Ungerstedt, 1990). By contrast, long-term potentiation (LTP) at corticostriatal synapses is nearly abolished in 6-OHDA-treated rats (Calabresi *et al*., 1996; Centonze *et al*., 1999), suggesting that changes in corticostriatal transmission contribute to basal ganglia dysfunctions in PD. However, the exact mechanisms that underlie these changes remain poorly understood. In addition to the neocortex, the thalamus is another significant source of glutamatergic inputs to the striatum (Charara *et al*., 2002; Smith *et al*., 2004), but regulatory changes of transmission along this system in PD have not been studied. It is, however, noteworthy that the centromedian/parafascicular (CM/PF) nuclear complex, one of the main sources of thalamic inputs to the striatum, shows a significant cell loss in post-mortem brains of PD patients (Henderson *et al*., 2000a,b). One may therefore hypothesize that both the corticostriatal and the thalamostriatal glutamatergic systems may be affected in PD.

The recent cloning of vesicular glutamate transporters (vGluT) 1 and 2 provides unique tools to differentiate cortical from thalamic axon terminals in the striatum. Studies from our laboratory and others have clearly shown that vGluT1 is confined to cortical boutons, whereas vGluT2 is a selective marker of thalamic afferents in the rat striatum (Lacey *et al*., 2005; Raju & Smith, 2005a; Fujiyama *et al*., 2006; Raju *et al*., 2006). In the present study, we took advantage of these selective markers to examine changes in distribution and relative abundance of cortical vGluT1-containing and thalamic vGluT2-containing terminals between control and methyl-4-phenyl-1,2,3,6-tetrahydropyridine (MPTP)-treated parkinsonian monkeys using

Correspondence: Dr Y. Smith, as above.
E-mail: ysmit01@emory.edu

Received 26 July 2007, revised 3 February 2008, accepted 7 February 2008

immunoelectron and confocal microscopic methods. To this end, we developed and characterized the specificity of a novel anti-vGluT2 antibody generated against the human vGluT2 sequence that recognizes monkey, but not rodent, vGluT2 protein. The present study demonstrates that striatal dopaminergic depletion results in an increased prevalence of vGluT1-containing corticostriatal terminals and a regional reorganization of the synaptic microcircuitry of vGluT2-containing thalamostriatal boutons in the caudate nucleus and putamen of MPTP-treated monkeys. These data demonstrate the high degree of glutamatergic synaptic plasticity in the striatum and raise questions about the differential roles of corticostriatal and thalamostriatal systems in normal and pathological basal ganglia function.

Materials and methods

Animals and tissue preparation

For Western immunoblots, brain tissue from one monkey and three rats were used. The monkey was overdosed with pentobarbital (100 mg/kg, i.v.), followed by rapid removal of the brain from the skull and dissection. The rodents were decapitated, and the brains were rapidly removed from the skull and dissected on ice.

For immunocytochemistry experiments, three rats, three control and three MPTP-treated adult Rhesus monkeys (*Macaca mulatta*) (Yerkes National Primate Research Center colony) were used. The rats were anesthetized with ketamine (60–100 mg/kg) and dormitor (0.1 mg/kg) and transcardially perfused with 40–50 mL of cold Ringer's solution followed by 400 mL of fixative containing a mixture of 4% paraformaldehyde and 0.1% glutaraldehyde in phosphate buffer (0.1 M, pH 7.4). After fixative perfusion, the brains were taken out from the skull and post-fixed in a 4% paraformaldehyde solution for 6–8 h at 4 °C.

Three monkeys (females, 5.68–6.42 kg, 4 years 7 months to 6 years 7 months) received weekly systemic i.v. injections of 0.3–0.7 mg/kg MPTP hydrochloride (Sigma-Aldrich, St Louis, MO, USA) in the saphenous vein over of period of 6–11 months to induce chronic parkinsonism, with at least 7 days between MPTP administrations. The monkeys received MPTP until they developed a moderate PD-like state that remained stable for a period of at least 6 months prior to perfusion. The degree of severity of the parkinsonian symptoms and general motor activity was assessed twice a month using the following methods. For general activity monitoring, the animals were transferred to an observation cage equipped with eight infrared beams (arranged in square configurations between back and front, and between the sides of the cage). The beam crossings were registered, time-stamped and stored to PC disk. This allowed us to calculate the number of activity counts/minute, and the total number of counts for longer time periods (e.g. per hour). To quantify parkinsonism, we used a modification of a rating scale developed by Kurlan *et al*. (1991). The overall score was composed of subscores for assessing posture (0–2), gait (0–4), bradykinesia (0–4), balance (0–2), gross motor skills (0–3) and defense reactions (0–2). Animals were categorized as mildly affected (summary score 0–6), moderately affected (6–12) or severely affected (12–17) based on their overall parkinsonian rating score. Two of the MPTP-treated monkeys used in this study were categorized as moderately affected (scores 10–12), while another animal reached a level of severe parkinsonism (score 13–15). Six to 8 months post-MPTP, the monkeys were deeply anesthetized with an overdose of pentobarbital and perfused transcardially with cold oxygenated Ringer's solution, followed by 2 L of fixative containing 4% paraformaldehyde and 0.1% glutaraldehyde in phosphate buffer (PB; 0.1 M, pH 7.4). After fixative perfusion, the brains were washed with PB, taken out from the skull and cut into 10-mm-thick blocks in the frontal plane. All animal procedures were performed according to the National Institutes of Health guide for the care and use of laboratory animals and have been reviewed by the Institutional Animal Care and Use Committee of Emory University. All efforts were made to reduce the number of animals used.

Tissue sections (60 μm thick) from both rat and monkey brains were obtained with a Vibratome, collected in cold phosphate-buffered saline (PBS; 0.01 M, pH 7.4), and treated with sodium borohydride (1% in PBS) for 20 min.

Generation and characterization of anti-vGluT2 antibody

Primary antisera

Three polyclonal antibodies were used, a guinea-pig anti-vGluT1 from Chemicon (Chemicon International, Temecula, CA, USA) generated against a 19-amino-acid sequence of the corresponding rat protein, a rabbit anti-vGluT1 from MabTechnologies (Atlanta, GA, USA) directed against amino acids 543–560 of rat protein and a new rabbit anti-human vGluT2 antibody (Mab Technologies). The specificity of the guinea-pig and rabbit anti-vGluT1 antibodies has been reported previously (Todd *et al*., 2003; Raju & Smith, 2005a; Villalba *et al*., 2006a).

For the new rabbit anti-vGluT2 antibody, a peptide was generated to the COOH terminus of the human vesicular glutamate transporter 2 (hvGluT2), corresponding to amino acids 560–578 (KKEEFVQGEVQDSHSYKDR). The underlined amino acids are human-specific. A cysteine was added to aid in conjugation to the protein carrier keyhole limpet hemocyanin (KLH; Pierce, Rockford, IL, USA). The antiserum was obtained from rabbits (Covance) immunized with the conjugated peptide and the IgG fraction was recovered by ammonium sulfate precipitation as follows: serum was first treated with 25% ammonium sulfate to remove any proteins that might precipitate at low ionic concentrations and incubated with stirring overnight at 4 °C. Following a 3000***g*** spin for 30 min, the supernatant was removed and transferred to a clean tube. Ammonium sulfate was added to a final concentration of 50% saturation. After another overnight incubation at 4 °C, the IgG fraction was isolated in the pellet by centrifugation at 3000 ***g*** for 30 min. The pellet was resuspended in PBS and dialysed overnight with three buffer changes. The specificity of vGluT2 antibody on monkey tissue was determined by Western immunoblots and light microscopy immunohistochemical analysis.

Western immunoblots

All brain membrane samples were prepared at 4 °C. After dissection, the striatal tissue was completely homogenized with a sonicator in an ice-cold buffer solution (20 mM HEPES, 10 mM EDTA, 2 mM Na_3VO_4). The homogenate was centrifuged for 5 min at 3000 ***g*** to remove tissue debris, and membranes were isolated from the supernatant by subsequent centrifugation for 30 min at 14 000 r.p.m. The resulting pellet was then solubilized in a buffer solution (20 mM HEPES and 0.1 mM EDTA) before total protein concentration was measured by using the Bio-Rad Protein Assay (Bio-Rad, Hercules, CA, USA). The homogenates were then centrifuged for 30 min at 14 000 r.p.m., and the pellet was solubilized in a lysis buffer [10 mM HEPES, 50 mM NaCl, 0.1 mM EDTA, 1 mM benzamidine, 1.0% Triton X-100, 0.1% SDS, protease inhibitor cocktail (one tablet per 50 mL; Roche Diagnostics GmbH, Mannheim, Germany)]. The lysates (5–10 μg protein) were then eluted with 1× SDS-PAGE sample buffer. The samples of brain tissue were resolved by SDS-PAGE and

subjected to Western blot analysis with anti-vGluT2 (0.2 μg/mL) antibody. Immunoreactive bands were detected with the enhanced chemiluminescence detection system (Pierce) with horseradish peroxidase-conjugated goat anti-rabbit secondary antibody (1 : 4000; Amersham Biosciences, Little Chalfont, UK).

Light microscopy analysis

To examine antibody specificity, preadsorption assays were performed by incubating anti-vGluT2 (0.04 μg/mL) primary antibodies with their corresponding peptides or heterologous synthetic peptides corresponding to the C-terminal of vGluT1 (2 μg/mL). The sections were preincubated in a solution containing 10% normal goat serum, 1% bovine serum albumin, and 0.3% Triton X-100 in PBS for 1 h. They were then incubated overnight with primary antisera diluted at 0.5–1.0 μg/mL in a solution containing 1.0% NGS, 1.0% BSA and 0.3% Triton X-100 in PBS. Next, the sections were rinsed in PBS and transferred for 1.5 h to a secondary antibody solution containing biotinylated goat anti-rabbit IgGs (Vector Laboratories, Burlingame, CA, USA) diluted 1 : 200 in the primary antibody diluent solution. After rinsing, sections were put in a solution containing 1% avidin–biotin–peroxidase complex (Vector). The tissue was then washed in PBS and 0.05 M Tris buffer before being transferred in a solution containing 0.01 M imidazole, 0.005% hydrogen peroxide and 0.025% 3,3′-diaminobenzidine tetrahydrochloride (Sigma) in Tris for 10 min. The DAB reaction was terminated with several rinses in PBS. The sections were then mounted onto gelatin-coated slides, dehydrated and a coverslip was applied with Permount. Selected fields of striatum were photographed with a Leica DC 500 digital camera.

Dopamine transporter immunostaining in MPTP-treated monkeys

To determine the extent of dopamine depletion, precommissural striatal tissue and midbrain sections from MPTP-treated monkeys were immunostained for dopamine transporter, using monoclonal rat anti-dopamine transporter IgGs (0.2 μg/mL; Chemicon; Catalog no. MAB369) (Miller *et al*., 1997). The immunolabeling protocol was identical to that used for the light microscopic localization of vGluT2 described above, except that the secondary antibody was a biotinylated goat anti-rat antibody (1 : 200 dilution; Vector Laboratories).

Immunoperoxidase electron microscopic localization of vGluT1 and vGluT2

The sections were placed in a cryoprotectant solution (PB; 0.05 M, pH 7.4, containing 25% sucrose and 10% glycerol) for 20 min, frozen at −80 °C for 20 min, thawed, and returned to a graded series of cryoprotectant (100, 70, 50 and 30%) diluted in PBS. They were then washed in PBS before being processed for immunocytochemistry.

Sections were incubated with rabbit anti-vGluT1 or vGluT2 antibodies and processed for immunoperoxidase localization in a manner identical to that for light microscopy, except that the incubation in the primary antisera was performed at 4 °C for 48 h and Triton X-100 was omitted from all incubation solutions. Sections were incubated with (i) rabbit anti-vGluT1 (0.2 μg/mL), (ii) rabbit anti-vGluT2 (0.2 μg/mL) or (iii) both primary antibodies.

Following the immunostaining reactions, the sections were transferred to PB (0.1 M, pH 7.4) for 10 min and exposed to 1% osmium tetroxide for 20 min. They were then rinsed with PB and dehydrated in an increasing gradient of ethanol. Uranyl acetate (1%) was added to the 70% alcohol to increase contrast at the electron microscope. The sections were then treated with propylene oxide before being embedded in epoxy resin (Durcupan, ACM; Fluka, Buchs, Switzerland) for 12 h, mounted on microscope slides, and placed in a 60 °C oven for 48 h.

Blocks of tissue from the precommissural and postcommissural caudate nucleus and putamen were taken out from the slides and glued on the top of resin blocks with cyanoacrylate glue. They were cut into 60-nm ultrathin sections with an ultramicrotome (Ultracut T2; Leica, Nussloch, Germany) and collected on single-slot Pioloform-coated copper grids. The sections were then stained with lead citrate for 5 min and examined with a Zeiss EM-10C electron microscope (Thornwood, NY, USA).

Control experiments

In a series of control experiments, sections were processed as described above without primary antibodies. The sections were completely devoid of immunostaining following these incubations.

Analysis of material

The number of animals and blocks and the total tissue area examined in each experimental group are given in Table 1. To ensure comparisons were made between the same striatal regions in normal and MPTP-treated monkeys, blocks were taken from corresponding regions of the pre- and postcommissural caudate nucleus and putamen in each experimental group. To minimize false negatives, only ultrathin sections from the most superficial sections of blocks were scanned at 25 000×. At the electron microscope, ultrathin sections were randomly scanned for the presence of immunoreactive terminals forming clear asymmetric synapses. These boutons were photographed and their postsynaptic targets were categorized as either dendrites or spines, based on ultrastructural criteria defined in Peters *et al*. (1991). Their relative proportion was calculated and expressed as a percentage (± SEM) of total labeled axon terminals expressing vGluT1 or vGluT2 from within each level of the caudate nucleus and putamen. The maximal diameter of immunolabled axon terminals was measured in parallel with the postsynaptic density, as previously described by Lei *et al*. (2004). Statistical differences in the percentage of axo-dendritic and axo-spinous synapses and the sizes of axon terminals and postsynaptic spines among all experimental groups were assessed using Kruskal–Wallis one-way ANOVA and subsequent Dunn's *posthoc* analysis (SigmaStat 3.0). All statistical differences were considered significant at $P < 0.05$. In cases involving axo-dendritic synapses, the diameter of axon terminals was included in the above measurements because no statistical difference was detected in the sizes of axon terminals forming axo-spinous or axo-dendritic synapses ($P = 0.5$). To compare the ratios of axo-spinous to axo-dendritic synapses in the different striatal regions, the Fisher's exact test was utilized with differences considered significant at $P < 0.05$.

To determine if prevalence of cortical and thalamic boutons changed in normal compared with MPTP-treated striata, a second

TABLE 1. Number of animals and blocks, and tissue area examined in each experimental group

	Animals (*n*)	Blocks (*n*)	Tissue area (μm^2)
vGluT1 control	3	6	10 460
vGluT1 MPTP	3	6	9960
vGluT2 control	3	6	9390
vGluT2 MPTP	3	6	9680

series of experiments was performed, in which all tissue sections incubated with vGluT1, vGluT2 or vGluT1 + vGluT2 antibodies were scanned at 12 500×. Elements were classified as labeled or unlabeled axon terminals forming asymmetric synapses and reported as a percentage (± SEM) of labeled terminals forming asymmetric synapses. Data from all striatal levels were collapsed to represent the entire striatum. Statistical differences in the pattern of distribution of the vGluTs between control and MPTP groups were assessed using the Mann–Whitney test with differences considered significant at $P < 0.05$.

Fluorescence confocal immunohistochemistry

Tissue sections from the precommissural and postcommissural striatal levels in both control and MPTP-treated brains were used to quantify the area of striatum occupied by vGluT1 immunofluorescence. All incubations were carried out at room temperature. After being cut at 60 μm on the vibratome, sections were incubated in sodium borohydride (1%) in PBS for 20 min and repeatedly rinsed in PBS. The sections were placed in a pre-incubation solution containing normal donkey serum (NDS; 5%), BSA (1%) and Triton-X (0.3%) for 1 h and then into an incubation solution containing guinea-pig anti-vGluT1 antibody (Chemicon; 0.2 μg/mL), NDS (1%) and BSA (1%) overnight and then washed in PBS. The sections were incubated in a solution containing Alex488-conjugated goat anti-guinea-pig IGs (5 μg/mL; Molecular Probes, Eugene, OR, USA; Catalog no. A11073), NDS (1%) and BSA (1%) for 1 h, rinsed in PBS, mounted with Vectashield (Vector Laboratories) and stored at 4 °C. Sections were scanned with a Leica TCS/SL laser scanning confocal microscope coupled to a Leica DMR-compatible axiovert and a 63× oil-immersion objective with sequential acquisition settings at the maximal resolution of the confocal (1024 × 1024 pixels). Final images were prepared using Adobe Phototoshop and adjusted for contrast and brightness.

Control experiments

Control incubations included omission of the vGluT1 primary antibodies while the rest of the procedure remained the same. These sections were completely devoid of immunostaining.

Quantification of vGluT immunoreactivity

For quantitative assessment of the vGluT1 immunofluorescence in the striatum, one to two sections of pre- and postcommissural striatal sections were selected from control ($n = 3$) and MPTP-treated ($n = 3$) monkeys, and five images were acquired from each level of the caudate nucleus and putamen. The observer (D.V.R.) was blinded to the identity of the tissue used (control vs. MPTP). With the chosen setting of the confocal system (5× digital zoom, pinhole 1.0), each image was a square with sides of 46 μm. Five such images were taken from each animal at different dorso-ventral levels of the caudate nucleus and putamen. Quantification was performed on unprocessed images with MetaMorph (version 6.1r4) imaging software (Universal Imaging Corp., West Chester, PA, USA). For each image, thresholding was performed to determine the level of fluorescence judged to accurately depict the size of stained structures. Three to six regions of interest within the striatum were selected from each image, and the area occupied by vGluT1 immunofluorescence was determined as a percentage of the total area of each region of interest. The data are presented as the mean percentage ± SEM. Statistical differences in percentages of area occupied by vGluT1 between control and MPTP groups within each level of the caudate nucleus and putamen were assessed using the Mann–Whitney test with differences considered significantly different at $P < 0.05$).

Results

Antibody specificity

The new anti-vGluT2 antibody generated against the C-terminus of the human vGluT2 protein uniquely immunolabels monkey, but not rat, vGluT2 protein (Fig. 1). Western blot analysis identified a single band at ∼65 kDa, as predicted for the vGluT2 protein in monkey but not in rat (Fig. 1A). Faint bands, at similar molecular weights, above and below the vGluT2 band were detected in lanes loaded with both monkey and rat tissue. These bands may reflect degradation products or non-specific background labeling. Further analysis at the light microscopic level confirmed the specificity of this antiserum. The neuropil was immunolabeled in monkey, but not in rat (Fig. 1B and C). Preadsorbtion of the antibody by control peptide abolished immunolabeling, whereas preincubation of the anti-vGluT2 antibody with vGluT1 peptide had no effect on the neuropil immunostaining (Fig. 1D and E). Omission of primary antibodies resulted in a complete abolition of neuropil immunostaining (Fig. 1F).

Dopamine depletion

Striatal dopamine depletion following MPTP administration was confirmed with DAT immunostaining (Fig. 2). Labeling for DAT was absent in the pre- and postcommissural striatum, except for small patches of DAT immunostaining in the medialmost parts of the caudate nucleus and putamen. The nucleus accumbens contained a

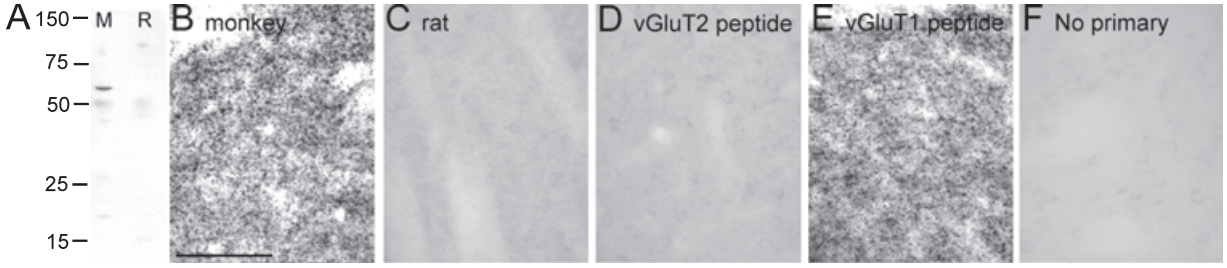

FIG. 1. vGluT2 antibody specificity. Western blot analysis with anti-vGluT2 antibody shows a prominent band in monkey (M), but not in rat (R), striatal tissue at ∼60 kDa corresponding to the molecular weight predicted for vGluT2. Faint bands were detected above and below the predicted vGluT2 band (A). Light microscopic examination with anti-vGluT2 antibodies demonstrates neuropil immunoreactivity in the monkey putamen (B), but not in the rat striatum (C). Immunolabeling in monkey striatum is abolished when antibodies are preadsorbed with their corresponding peptides (D), but is preserved when antibodies are preadsorbed with a synthetic peptide corresponding to the C-terminal sequence of vGluT1 (E). Immunostaining of monkey striatal tissue without primary antibodies is shown for reference (F). Molecular weight standards are indicated on the left in kDa (A). Scale bar = 200 μm (applies to B–F).

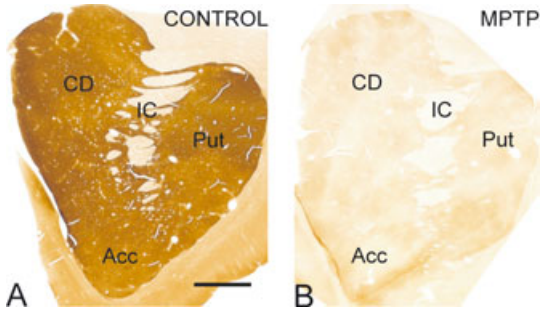

FIG. 2. Striatal dopamine transporter immunoreactivity following MPTP-induced nigrostriatal dopamine lesions. Immunoreactivity for dopamine transporter is nearly completely abolished in MPTP-treated (B) striatum of a severely affected parkinsonian monkey compared with controls (A). Sections of the precommissural striatum are shown. Scale bar represents 2 mm for both images.

thin diagonal strip of immunolabeling. The subtantia nigra pars compacta was nearly devoid of DAT labeling, except for faint immunoreactivity in its medialmost part and the ventral tegmental area (VTA) (not shown).

Localization of vGluT1 and vGluT2 terminals in normal and MPTP striata

Knowing that glutamatergic inputs to different striatal regions largely arise from specific cortical and thalamic nuclei (Parent & Hazrati, 1995; Smith *et al*., 2004), combined with the fact that the postcommissural putamen is more sensitive than other striatal regions to dopamine depletion (Perez-Otano *et al*., 1994), we compared the synaptic organization and relative abundance of vGluT1- and vGluT2-containing terminals between pre- and postcommissural levels of the caudate nucleus and putamen in normal and MPTP-treated monkeys. Irrespective of the striatal areas examined, more than 95% of vGluT1-immunolabeled terminals formed axo-spinous synapses in both control and MPTP conditions (Figs 3A and D, and 4A and B). In contrast, vGluT2-immunolabeled terminals formed synapses onto dendrites and spines in about the same proportion at all striatal levels in control tissue (Figs 3B, C, E and F, and 4C and D). Despite an apparent increase in the ratio of vGluT2-containing axo-spinous to axo-dendritic synapses in the pre-caudate and post-putamen striatal regions of MPTP-treated monkeys, these changes were not found to be statistically significant (Fisher's exact test; $P = 0.114$), as was the case for other striatal areas (Fig. 5).

Morphological differences between vGluT1 and vGluT2 terminals in normal and MPTP striata

VGluT1- and vGluT2-containing boutons displayed common ultrastructural features, i.e. both types of axon terminals were densely packed with round, electron-lucent vesicles and formed asymmetric synapses with thick presynaptic densities (Fig. 3A–F).

In order to assess potential morphological differences in vGluT1- and vGluT2-containing terminals between normal and MPTP conditions and to compare the size of the boutons with that previous reported for corticostriatal boutons in rats (Lei *et al*., 2004), we measured the cross-sectional diameter of a large pool of vGluT1- and vGluT2-immunostained terminals at various striatal levels in normal and MPTP-treated monkeys. No significant difference was found between the diameters of vGluT1- and vGluT2-immunoreactive boutons in both normal and MPTP conditions (Fig. 3G).

Relative abundance of vGluT1- and vGluT2-containing terminals in striata of normal vs. MPTP-treated monkeys

To assess whether dopamine depletion had an effect on the relative abundance of vGluT1- and vGluT2-containing terminals in the striatum, immunoreactive and non-immunoreactive terminals forming asymmetric synapses were counted from the surface of a large sample of pre- and postcommissural striatal sections immunostained for vGluT1 or vGluT2. VGluT2-containing boutons accounted for about the same proportion of glutamatergic terminals in both the striatum of control (21.7 ± 1.3%; $n = 1616$ terminals forming asymmetric synapses) and MPTP-treated (21.5 ± 1.2%; $n = 1534$) monkeys (Fig. 6). In contrast, there was a significant increase ($P = 0.007$) in the relative percentage of vGluT1-immunoreactive boutons in MPTP (66.5 ± 3.4%; $n = 1327$) vs. control (51.9 ± 3.5%; $n = 1619$) conditions (Fig. 6).

To determine the overall proportion of glutamatergic terminals that express vGluT1 and vGluT2 in the striatum of naive and MPTP-treated monkeys, striatal tissue was incubated with a cocktail of both vGluT antibodies and the proportion of labeled vs. unlabeled boutons forming asymmetric synapses was determined from superficial ultrathin sections of striatal tissue where there is optimal penetration of both antibodies. In control and MPTP striatal tissues, both vGluT antibodies immunolabeled, respectively, 78.9 ± 3.208% ($n = 1608$) and 84.2 ± 1.748% ($n = 2127$) of all axon terminals forming asymmetric synapses (Fig. 6). No significant differences were found between the groups ($P = 0.335$).

VGluT1 immunofluorescence in striata of normal vs. MPTP monkeys

To characterize changes in the prevalence of vGluT1-immunoreactive terminals between control and MPTP-treated striata further, we quantified the relative area of striatum occupied by vGluT1 immunofluorescence in different sections of pre- and postcommissural caudate nucleus and putamen of normal and MPTP-treated monkeys (Fig. 7). In line with the electron microscopic data, vGluT1 immunofluorescence occupied a significantly larger area of the striatal tissue in MPTP-treated monkeys than in controls ($P < 0.01$).

Discussion

The present study provides evidence for differential effects of midbrain dopamine depletion on the two main glutamatergic pathways to the striatum in the MPTP-treated monkey model of PD. Four main conclusions can be drawn from our findings. First, vGluT1-containing corticostriatal afferents and vGluT2-containing thalamostriatal terminals display strikingly different patterns of synaptic organization in the monkey striatum. Second, chronic MPTP treatment leads to significant increases in the relative proportion of vGluT1-immunoreactive terminals, but not vGluT2-containing boutons, in the monkey striatum. Third, midbrain dopamine depletion induced by chronic MPTP injections results in significant changes in the ratio of axo-spinous to axo-dendritic synapses formed by vGluT2-containing terminals in the precommissural caudate nucleus and postcommissural putamen. Fourth, almost 20% of terminals forming asymmetric synapses in the monkey striatum do not express vGluT1 or vGluT2, suggesting that another vGluT isoform or neurotransmitter is used by these boutons.

Together, these findings provide further evidence for the significant difference in the synaptic microcircuitry of cortical vs. thalamic glutamatergic afferents to the monkey striatum and demonstrate that

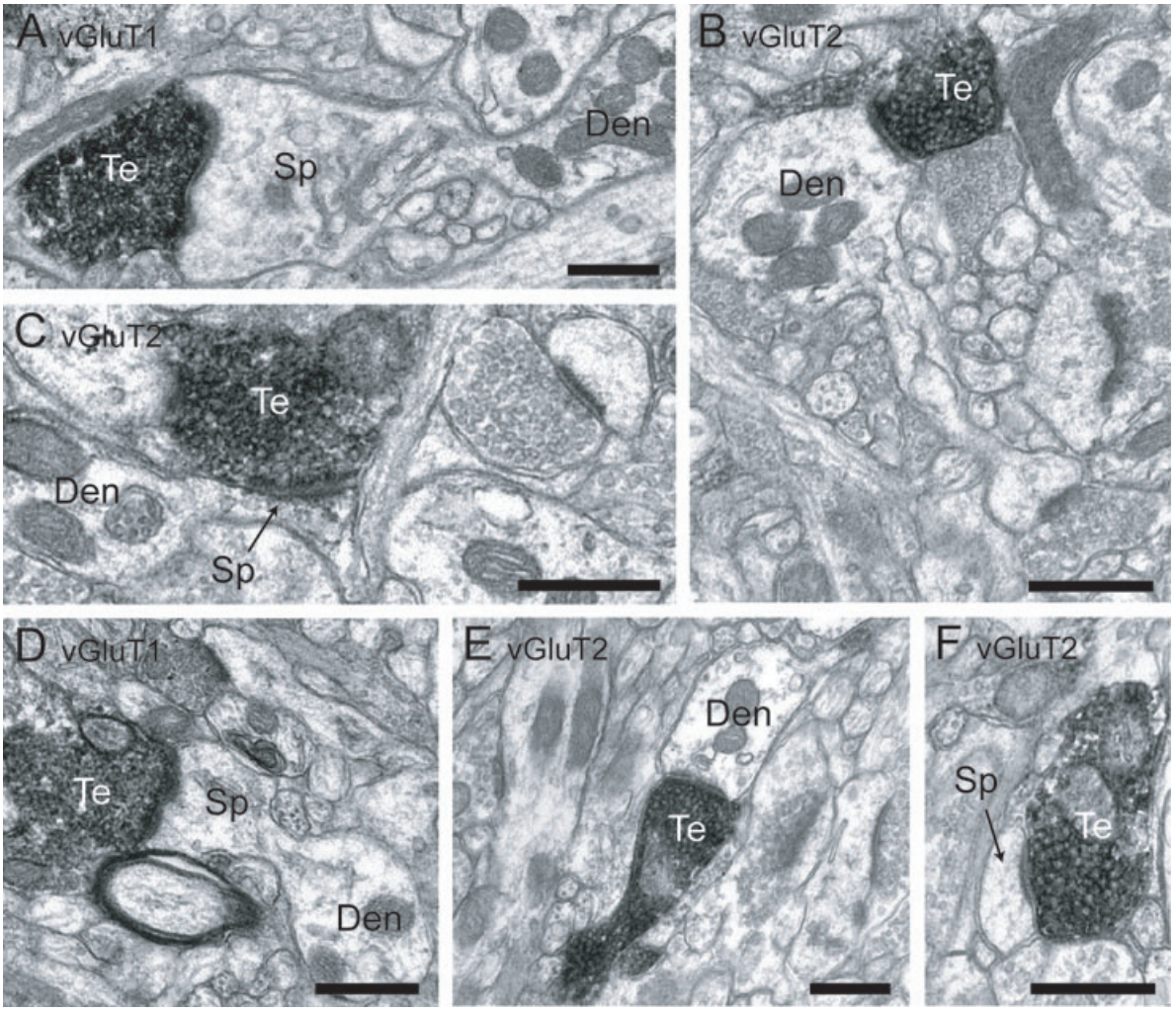

G

	Control		MPTP	
	vGluT1 (mean ± SEM)	vGluT2 (mean ± SEM)	vGluT1 (mean ± SEM)	vGluT2 (mean ± SEM)
Terminal Size (mm)	0.783 ± 0.0154 (n=341)	0.759 ± 0.0141 (n=337)	0.795 ± 0.0145 (n=317)	0.777 ± 0.0164 (n=361)

FIG. 3. vGluT1 and vGluT2 immunoreactivity in the striatum of control and MPTP-treated monkeys. Axon terminals immunolabeled for vGluT1 form axo-spinous synapses in both control (A) and MPTP-treated (D) monkeys. Axon terminals immunolabeled for vGluT2 terminate onto dendritic shafts and spines in both control (B and C) and MPTP-treated monkeys (E and F). Te, axon terminal; Den, dendrite; Sp, spine. (G) The size of vGluT1- and vGluT2-immunolabeled terminals was not significantly different between control and MPTP-treated monkeys ($P = 0.502$). Sizes (μm) are reported as mean ± SEM; n = number of terminals measured. Statistical differences were determined by Kruskal–Wallis one-way analysis of variance on ranks with Dunn's *posthoc* test. Scale bars represent 0.5 μm for all images.

dopamine depletion involves complex reorganization of this striatal microcircuitry of glutamatergic afferents in parkinsonism.

Specificity of vGluT1 and vGluT2 antibodies

A novel antibody against the human vGluT2 protein has been generated and characterized. Several commercially available antibodies generated against rat vGluT2 were initially examined (Chemicon, Sigma and Synaptic Systems, Mab Technologies) but none showed specific immunolabeling (data not shown). This lack of labeling was likely due to the significant difference in amino-acid sequence of the C-terminal between rats and primates (73% homology). Several lines of evidence support the specificity of the human anti-vGluT2 antibody used in the present study. First, a BLAST search yielded no matches to vGluT1, vGluT3 or other known proteins localized in axon terminals, but showed greater homology to the predicted chimpanzee vGluT2 sequence (100% to amino acids 693–711) than the corresponding rat sequence (73% to amino acids 560–578). Second, immunolabeling in both Western blot and immunocytochemistry showed immunoreactivity

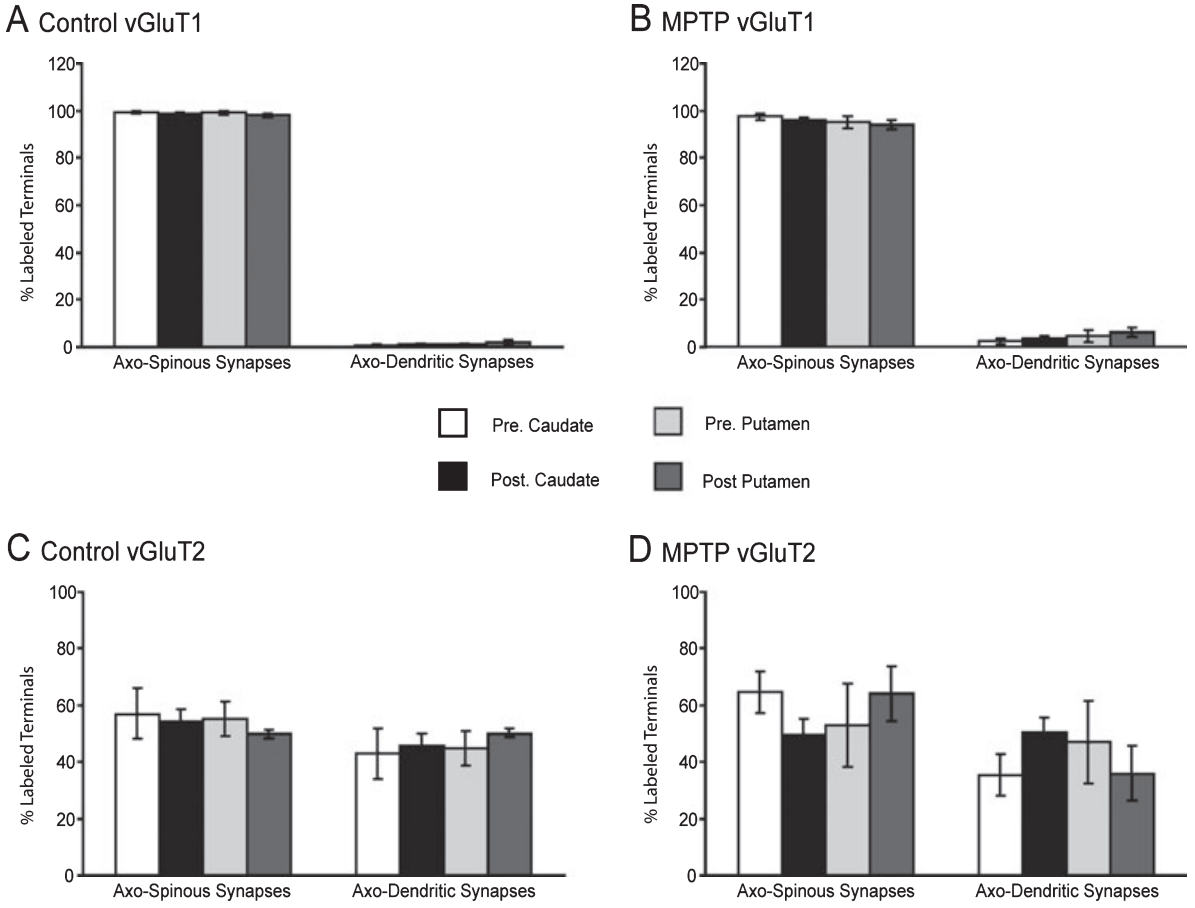

FIG. 4. Synaptology of vGluT1- and vGluT2-labeled terminals at different striatal levels of control and MPTP-treated monkeys. VGluT1-containing terminals form significantly more axo-spinous synapses at all striatal levels in both control (A) and MPTP (B) conditions ($P < 0.05$). VGluT2-containing terminals form axo-dendritic and axo-spinous synapses in both control (C) and MPTP (D) states. VGluT2-containing terminals form significantly ($P = 0.046$) more axo-spinous synapses than axo-dendritic synapses in the precommissural caudate nucleus of MPTP-treated monkeys. No other significant difference was detected in the proportion of axo-dendritic and axo-spinous synapses at other striatal levels in either control or MPTP-treated monkeys.

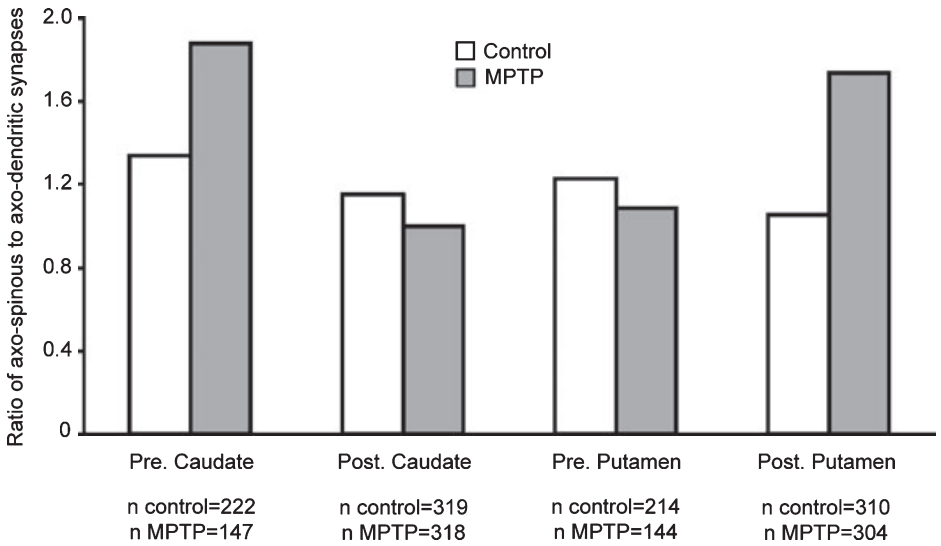

FIG. 5. Thalamostriatal reorganization in MPTP-treated monkeys. The ratio of axo-spinous to axo-dendritic vGluT2-containing synapses was not significantly different between pre- and postcommissural levels of the caudate nucleus and putamen in controls, but the ratio significantly ($P < 0.05$) decreased between the pre- and postcommissural caudate nucleus and significantly ($P < 0.05$) increased between the pre- and postcommissural putamen in MPTP-treated monkeys. Statistical differences were determined by Fisher's exact test. n indicates the total number of terminals examined in each striatal region in both control and MPTP-treated monkeys.

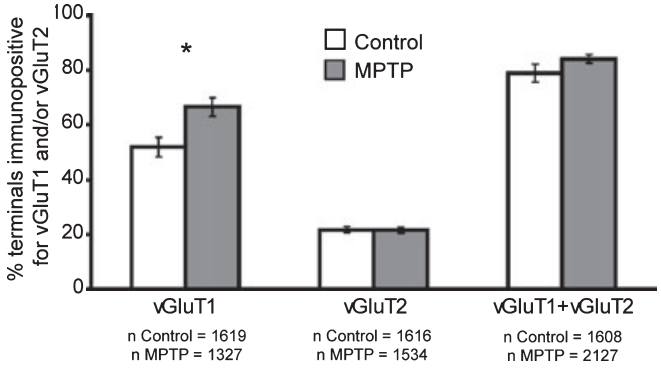

FIG. 6. Proportion of axon terminals forming asymmetric synapses labeled for vGluT1, vGluT2 or both transporters. The percentage of vGluT1-immunolabeled axon terminals forming asymmetric synapses was significantly larger in the striatum of MPTP-treated monkeys than in controls (*$P = 0.007$). Values reported are the number of vGluT1-, vGluT2- or vGluT1 + vGluT2-immunoreactive terminals expressed as the percentage (± SEM) of the total number of terminals forming asymmetric synapses in the caudate nucleus and putamen; n is the total number of terminals forming asymmetric synapses. Three control and three MPTP-treated monkeys were used. Statistical differences were determined by using the Mann–Whitney rank sum test, and statistical significance was set at $P < 0.05$.

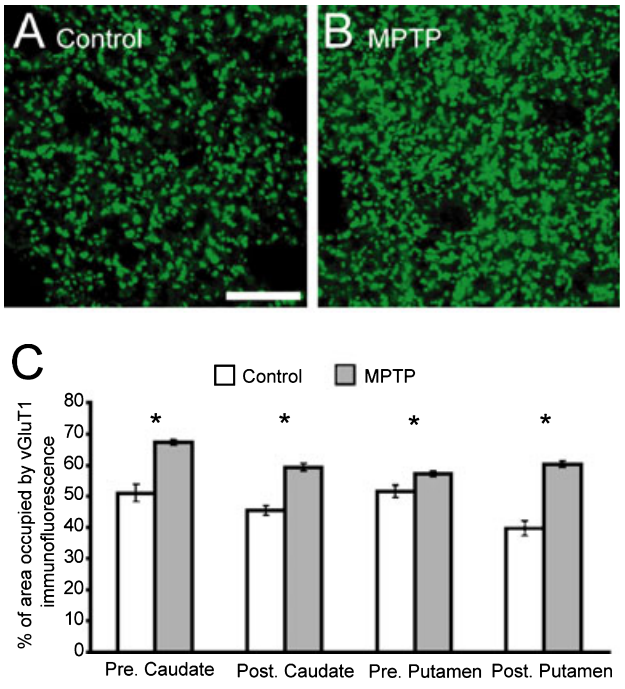

FIG. 7. vGluT1 immunofluorescence in the striatum of control vs. MPTP-treated monkeys. Immunofluorescence for vGluT1 in the postcommissural putamen of control (A) vs. MPTP-treated monkeys (B). The striatal area occupied by vGluT1 immunofluorescence is significantly (*$P < 0.05$) higher at all levels of the caudate nucleus and putamen in MPTP-treated monkeys compared with controls (C). Statistical differences were determined by using the Mann–Whitney test. Scale bar represents 10 μm for both A and B.

in monkey, but not in rat, striatal tissue. This indicates that the antibody recognizes the monkey, but not the rat, vGluT2 protein (Fig. 1). Thirdly, preadsorbtion with the control peptide, but not a sequence of the vGluT1 C-terminal peptide, abolished immunolabeling in monkey tissue. Finally, immunoperoxidase for vGluT2 in the monkey striatum is restricted exclusively to axon terminals and preterminal vesicle-filled unmyelinated axon segments, a pattern similar to that previously reported in rat (Lacey *et al*., 2005; Raju & Smith, 2005a). The specificity of anti-vGluT1 antibodies in our study has been thoroughly characterized in previous studies in our laboratory and others (Todd *et al*., 2003; Montana *et al*., 2004; Raju & Smith, 2005a). Based on these observations, we are confident that the anti-vGluT1 and anti-vGluT2 antibodies used in the study are highly specific and can be considered as selective markers of glutamatergic afferents in the monkey striatum.

Differential synaptology of vGluT1- and vGluT2-containing terminals in monkey striatum

A striking finding of the present study is the difference in the synaptology of vGluT1- and vGluT2-positive terminals. At all levels of the caudate nucleus and putamen, vGluT1-containing terminals almost exclusively targeted dendritic spines, whereas a very small proportion (2–6%) formed axo-dendritic synapses. By contrast, vGluT2-labeled terminals contacted both dendritic shafts and spines, with a slight preference toward axo-spinous synapses at most striatal levels. The preferential targeting of dendritic spines by vGluT1-positive terminals is consistent with similar studies in the rat striatum, showing that more than 95% of vGluT1-positive terminals form axo-spinous synapses (Lacey *et al*., 2005; Raju & Smith, 2005a; Raju *et al*., 2006). In contrast, another study of the rat striatum revealed that only about 80% of vGluT1-immunolabeled axon terminals innervate spines (Fujiyama *et al*., 2006). The sensitivity of vGluT1 antibodies, slight differences in quantitative methods and potential species differences between primate and non-primates may account for the discrepancy in the proportion of vGluT1-containing terminals in the rat vs. monkey striatum.

Recent studies from our laboratory and others reported that almost 80% of vGluT2-containing terminals contact dendritic spines in the rat striatum (Lacey *et al*., 2005; Raju *et al*., 2006). These findings are different from those of the present study showing that only 50–65% of vGluT2-containing boutons form axo-spinous synapses in the monkey striatum. These results highlight a potential species difference in the synaptic connectivity of vGluT2-containing terminals between rodent and monkey striata. It is possible that the CM/PF thalamostriatal projection accounts for a larger proportion of synapses formed by vGluT2-immunoreactive terminals in the monkey striatum compared with the striatal projections from PF in rats, thereby contributing to the larger percentage of axo-dendritic synapses in monkeys. By contrast, the striatal afferents from thalamic nuclei, other than the PF, which form almost exclusively axospinous sysnapses in rats (Raju *et al*., 2006), may represent a larger proportion of vGluT2-immunoreactive terminals that target dendritic spines in rats compared with monkeys.

Although vGluT1 and vGluT2 are selective markers of corticostriatal and thalamostriatal systems, respectively, they are pharmacologically similar and both confer glutamatergic activity to neurons (Bellocchio *et al*., 2000; Takamori *et al*., 2000, 2001). A fundamental difference between the two transporters is their complementary distribution in the brain (Hisano *et al*., 2000, 2002; Aihara *et al*., 2001; Fremeau *et al*., 2001, 2004; Herzog *et al*., 2001). *In situ* hybridization for vGluT1 and vGluT2 mRNA shows that vGluT1 signal predominates in all areas of the cerebral cortex, except for layer IV of the frontal, parietal and temporal cortices (Fremeau *et al*., 2001, 2004; Herzog *et al*., 2001). Because cortical neurons in layers III and V, which primarily express vGluT1 mRNA, project to the striatum, it is likely that corticostriatal afferents utilize vGluT1 (Charara *et al*.,

2002; Smith *et al*., 2004). On the other hand, vGluT2 mRNA is most abundant in the thalamus (Hisano *et al*., 2000; Aihara *et al*., 2001; Fremeau *et al*., 2001, 2004; Herzog *et al*., 2001). In fact, no vGluT1 mRNA was detected in the human thalamus (Aihara *et al*., 2001), but such is not the case in rats where a moderate expression level of vGluT1 was found in principal relay and association thalamic nuclei (Barroso-Chinea *et al*., 2007). A recent study combining retrograde labeling and *in situ* hybridization for vGluT2 mRNA in the rat showed that almost 99% of all retrogradely labeled thalamocortical neurons express vGluT2 mRNA (Hur & Zaborszky, 2005), and lesions of intralaminar thalamic nuclei significantly reduced intrastriatal vGluT2 expression in rat (Bacci *et al*., 2004). Furthermore, vGluT1 and vGluT2 identify segregated populations of axon terminals. Double immunoperoxidase and immunogold labeling for vGluT1 and vGluT2 in the rat striatum identified about 1% of all labeled terminals as doubly labeled for both transporters (Raju & Smith, 2005a). Immunofluorescence for both transporters identified no colocalization in the rat striatum (Lacey *et al*., 2005). Data presented in the present study further support a high level of segregation between vGluT1 and vGluT2 in the striatum of normal and MPTP-treated monkeys. The fact that the cocktail of vGluT1 and vGluT2 antibodies labeled a total proportion of terminals (79% in normal; 84% in MPTP) that closely corresponded to the addition of terminals labeled for vGluT1 (52% in normal; 66% in MPTP) + terminals labeled for vGluT2 (22% in both normal and MPTP) in single labeled sections confirms the lack of significant colocalization of the two transporters in both normal or pathological conditions. Together, these results indicate that, in both primates and non-primates, vGluT1 and vGluT2 are selective markers of the corticostriatal and thalamostriatal afferents, respectively.

The finding that vGluT1-positive terminals form mostly axo-spinous synapses is in agreement with several lesion and anterograde tracing studies of corticostriatal afferents in both rats and monkeys, showing that the majority of corticostriatal axon terminals contact dendritic spines (Kemp & Powell, 1971; Dube *et al*., 1988; Lapper & Bolam, 1992; Smith *et al*., 2004; Raju & Smith, 2005a). By contrast, the small population of vGluT1-containing terminals that synapse onto dendritic shafts is likely targeting preferentially parvalbumin-containing GABAergic interneurons, which were found to receive a significant cortical input in rodents (Lapper *et al*., 1992). Other interneurons, which also receive sparse cortical afferents (Wilson *et al*., 1990; Lapper *et al*., 1992; Bennett & Bolam, 1994; Berretta *et al*., 1997; Parthasarathy & Graybiel, 1997), may also account for the small population of vGluT1-containing axo-dendritic synapses.

However, the differential innervation of dendritic spines and shafts by vGluT2-labeled terminals raises several interesting possibilities regarding the overall synaptology of the thalamostriatal system. Much of our understanding of the thalamostriatal circuitry in monkeys comes from extensive studies of striatal projections from the CM/PF, showing that afferents from this nuclear complex predominantly (66–81%) innervate dendritic shafts (Sadikot *et al*., 1992). Although a large proportion of vGluT2-labeled terminals form axo-dendritic synapses, the slightly larger population of axo-spinous synapses strongly suggests that thalamostriatal afferents from other nuclei innervate dendritic spines of medium spiny neurons. Indeed, large lesioning studies of the thalamus have identified anterogradely degenerating axon terminals that contact dendritic spines (Kemp & Powell, 1971) in monkeys. Moreover, recent anterograde labeling studies in our laboratory revealed that over 90% of axon terminals originating for the central lateral, midline, mediodorsal, anteroventral, lateral dorsal and ventral anterior/ventral lateral thalamic nuclei terminate onto dendritic spines, whereas almost 90% of boutons from the PF target dendritic shafts (Raju *et al*., 2006), suggesting that PF afferents are unique in their preferential innervation of dendritic shafts. In addition to medium spiny neurons, CM/PF thalamostriatal afferents target cholinergic, parvalbumin-containing and somatostatin-containing, but not calretinin-positive, interneurons in monkeys (Sidibe & Smith, 1999). The possibility that vGluT2-labeled terminals differentially innervate striatal interneurons awaits further investigation.

Changes in the prevalence of vGluT1-containing terminals in the striatum of MPTP-treated monkeys

Another key finding of the present study is the significant increase in the percentage of vGluT1-labeled terminals in the striatum of MPTP-treated monkeys compared with controls. In light of the evidence that vGluT1-positive terminals form primarily axo-spinous synapses, these results strongly suggest that corticostriatal innervation, and likely neurotransmission, is significantly increased in the MPTP state. It is well established that nigrostriatal dopamine depletion leads to complex neurochemical and morphological changes within the basal ganglia circuitry in PD (Albin *et al*., 1989, 1995; Crossman, 1989; DeLong, 1990). In the striatum, there is evidence for an increased level of extracellular glutamate in 6-OHDA-treated rats (Lindefors & Ungerstedt, 1990). The diameter of the postsynaptic density of glutamatergic axo-spinous synapses is increased in the same animal model (Ingham *et al*., 1993; Meshul *et al*., 2000), suggesting that corticostriatal activity may, indeed, be increased in PD. In line with these observations, there is a significant increase in the percentage of neurons exhibiting spontaneous excitatory depolarizing potentials, which are blocked by AMPA glutamate receptor antagonists (Calabresi *et al*., 1993) in 6-OHDA-lesioned rats. There is also evidence for increased corticostriatal activity, in MPTP-treated monkeys. For example, striatal expression of the NR1 subunit of the NMDA receptor is down-regulated, likely in response to increased glutamatergic transmission (Betarbet *et al*., 2004). Administration of certain NMDA receptor antagonists reduces dyskinesias brought on by L-DOPA in parkinsonian monkeys (Papa & Chase, 1996; Blanchet *et al*., 1998, 1999). In light of these findings, the increased immunoreactivity for vGluT1 described in our study provides a substrate for increased corticostriatal activity in MPTP-treated monkeys. It is noteworthy that our data are in line with recent findings from post-mortem human brain tissue showing increased vGluT1 protein level in the putamen of parkinsonian humans (Kashani *et al*., 2007). Recent evidence that the level of vGluT1 can directly affect presynaptic quantal size (Wojcik *et al*., 2004; Wilson *et al*., 2005) lends support to the possibility that increased vGluT1 expression contributes to enhanced corticostriatal transmission.

However, these results are paradoxical in light of evidence that 17–27% of dendritic spines are lost in striata of 6-OHDA-treated rats, reserpine-treated mice and PD patients (Ingham *et al*., 1998; Stephens *et al*., 2005; Day *et al*., 2006). Furthermore, a recent study from our laboratory showed as much as 50% spine loss in the postcommissural putamen of MPTP-treated monkeys (Villalba *et al*., 2006b). It is worth noting, however, that these studies show a loss of dendritic spines, but do not directly assess the number of corticostriatal boutons. Corticostriatal afferents mostly form axo-spinous synapses, and if there is strict one-to-one pairing of afferents and spines then a loss of dendritic spines should lead to a reduction in the relative proportion of vGluT1-positive terminals in the striatum. Reconciling the discrepancy of spine loss with increased striatal glutamatergic neurotransmission suggests that the remaining striatal spines are more excitable after dopamine depletion in rats (Lindefors & Ungerstedt, 1990; Calabresi *et al*., 1993; Meshul *et al*., 2000; Day *et al*., 2006). A potential

mechanism to explain the increase in corticostriatal innervation despite a reduction in the number of spines is that as a result of remodeling after dopamine depletion, the remaining dendritic spines may receive contact from multiple vGluT1-containing terminals. Three-dimensional reconstruction of vGluT1-containing axo-spinous synapses in MPTP-treated monkeys is currently underway to determine the number of vGluT1-immunoreactive axon terminals that innervate single dendritic spines in normal and MPTP-treated monkeys. Another possibility could be that the increased density of vGluT1-immunoreactive terminals in the striatum of MPTP-treated monkeys was the result of reduced striatal volume in parkinsonian monkeys. Although this was not directly assessed in the present study, qualitative observations of the caudate nucleus and putamen in our material and others do not suggest any significant change in the striatal volume of MPTP-treated monkeys (see Fig. 2; Elsworth *et al*., 1996; Eberling *et al*., 1999; Palfi *et al*., 2002; Villalba *et al*., 2006b), but this remains to be confirmed quantitatively using the Cavalieri principle.

Reorganization of the microcircuitry of vGluT2-containing terminals in the striatum of MPTP-treated monkeys

Although no significant difference in the relative abundance of vGluT2-containing terminals was detected between control and MPTP-treated monkeys, the proportion of vGluT2-containing terminals targeting dendritic shafts vs. spines significantly changed in the striatum of MPTP-treated monkeys. Interestingly, this change occurred only in specific rostrocaudal levels of the caudate nucleus and putamen. In MPTP-treated monkeys, the ratio of axo-spinous to axo-dendritic vGluT2-containing synapses was significantly larger in the precommissural caudate nucleus than in the postcommissural counterpart, whereas it was significantly increased in the postcommissural putamen than in the precommissural putamen, suggesting a differential remodeling of the microcircuitry of the thalamostriatal system in specific striatal regions in response to dopamine depletion (Perez-Otano *et al*., 1994). In contrast, this ratio remained fairly constant throughout the rostrocaudal extent of the caudate nucleus in normal monkeys.

Although we have no clear explanation for this regional change in the synaptology of vGluT2-containing terminals at different striatal levels, one may consider the possibility that dopamine denervation leads to the loss of specific subpopulations of dendritic spines, some being targeted by thalamic inputs, at different levels of the striatum (Ingham *et al*., 1998; Stephens *et al*., 2005), which may contribute to the reorganization of vGluT2-containing synapses. Indeed, recent observations from our laboratory have revealed a significant difference in the extent of spine loss in the postcommissural compared with the precommissural striatum of MPTP-treated monkeys (Villalba *et al*., 2006b). This regional loss partly explains the significantly lower ratio of axo-spinous to axo-dendritic synapses in the postcommissural caudate nucleus of MPTP-treated monkeys, suggesting that as spines are lost, thalamostriatal afferents may preferentially target dendritic shafts. This observation may also be partly explained by a selective loss of thalamostriatal afferents that target the postcommissural caudate nucleus. It is noteworthy that 50–70% of CM/PF neurons degenerate in post-mortem tissue from patients with PD (Henderson *et al*., 2000a,b), and nearly 70% of thalamostriatal neurons originating in the PF are lost in 6-OHDA-treated rats (Aymerich *et al*., 2006). Although CM/PF degeneration has not been reported in the MPTP monkey model of PD, such a process may contribute to the reorganization of thalamostriatal innervation following nigrostriatal dopamine depletion. The complex interaction of regional spine loss and CM/PF neuronal cell loss may underlie the significantly higher ratio of axo-spinous to axo-dendritic synapses in the postcommissural putamen compared with the precommissural putamen of MPTP-treated monkeys.

Putative glutamatergic terminals devoid of vGluT1 and vGluT2 immunoreactivity

Immunolabeling for both vGluT1 and vGluT2, which is thought to label the total glutamatergic innervation of the dorsal striatum, revealed that about 15–20% of all axon terminals forming asymmetric synapses were not labeled for either transporter in the monkey striatum. These results are similar to those obtained in the rat striatum, which showed that about 30% of terminals forming asymmetric synapses do not express either transporter (Lacey *et al*., 2005). Virtually all asymmetric synapses in the dorsal striatum are thought to be excitatory and glutamatergic, while other chemical inputs that have been examined so far form predominantly symmetric synapses (Smith & Bolam, 1990). Three possibilities can be suggested to explain the significant number of unlabeled glutamatergic terminals: (i) the amount of vGluT1 or vGluT2 in some synapses falls below levels that can be detected reliably with the immunoperoxidase method; (ii) the level of vGluT1 and vGluT2 protein expression is dynamically up- or down-regulated, depending on physiological demands; and (iii) these axon terminals may express another vGluT, such as vGluT3 or a yet to be identified transporter (Gras *et al*., 2002). However, vGluT3 is an unlikely candidate because it is primarily expressed in postsynaptic spines and dendrites (Fremeau *et al*., 2002, 2004; Harkany *et al*., 2003). Although vGluT3 is partly coexpressed in striatal cholinergic terminals (Gras *et al*., 2002), these are unlikely to account for these unlabeled boutons because cholinergic terminals mainly form symmetric axo-dendritic synapses in the striatum (Smith & Bolam, 1990). It is noteworthy that the proportion of unlabeled axon terminals is not significantly different between the control and MPTP conditions, suggesting that the increase in the prevalence of vGluT1-positive terminals in MPTP-treated striata is not the result of novel vGluT1 expression in a population of previously unlabeled axon terminals. Future studies are needed to clarify this issue.

Concluding remarks

VGluT1 and vGluT2 are powerful tools to identify cortical and thalamic glutamatergic afferents to the monkey striatum. The significant difference in the pattern of synaptic organization of these two systems highlights their high degree of specificity in the striatal microcircuitry. The substantial increase in corticostriatal innervation and significant changes in the synaptic connectivity of the thalamostriatal system in MPTP-treated monkeys may either contribute to the pathophysiology of PD or serve as an adaptive mechanism to compensate for striatal dopamine loss. Together, these findings provide further evidence for a significant level of synaptic plasticity in the monkey striatum and pave the way for development of a better understanding of the neurochemical and morphological changes that underlie PD pathophysiology.

Acknowledgements

This study was supported by grants from the NIH to Y.S., R.A.H. and D.G.S. and the Yerkes National Primate Research Center NIH base grant (RR 00165). R.A.H. is also supported by a Distinguished Young Scholar in Medical Research Award from the W.M. Keck Foundation. We thank Craig Heilman and MAbTechnologies for the development of the vGluT2 antiserum. We are also grateful to Jean-Francois Pare and Susan Jenkins for technical support.

Abbreviations

6-OHDA, 6-hydroxydopamine; CM/PF, centromedian/parafascicular nuclear complex; hvGluT2, human vesicular glutamate transporter 2; MPTP, methyl-4-phenyl-1,2,3,6-tetrahydropyridine; NDS, normal donkey serum; PB, phosphate buffer; PBS, phosphate-buffered saline; PD, Parkinson's disease; vGluT, vesicular glutamate transporter.

References

Aihara, Y., Onda, H., Teraoka, M., Yokoyama, Y., Seino, Y., Kasuya, H., Hori, T., Tomura, H., Inoue, I., Kojima, I. & Takeda, J. (2001) Assignment of SLC17A6 (alias DNPI), the gene encoding brain/pancreatic islet-type Na^+-dependent inorganic phosphate cotransporter to human chromosome 11p14.3. *Cytogenet. Cell Genet.*, **92**, 167–169.

Albin, R.L., Young, A.B. & Penney, J.B. (1989) The functional anatomy of basal ganglia disorders. *Trends Neurosci.*, **12**, 366–375.

Albin, R.L., Young, A.B. & Penney, J.B. (1995) The functional anatomy of disorders of the basal ganglia. *Trends Neurosci.*, **18**, 63–64.

Anglade, P., Mouatt-Prigent, A., Agid, Y. & Hirsch, E. (1996) Synaptic plasticity in the caudate nucleus of patients with Parkinson's disease. *Neurodegeneration*, **5**, 121–128.

Aymerich, M.S., Barroso-Chinea, P., Perez-Manso, M., Munoz-Patino, A.M., Moreno-Igoa, M., Gonzalez-Hernandez, T. & Lanciego, J.L. (2006) Consequences of unilateral nigrostriatal denervation on the thalamostriatal pathway in rats. *Eur. J. Neurosci.*, **23**, 2099–2108.

Bacci, J.J., Kachidian, P., Kerkerian-Le Goff, L. & Salin, P. (2004) Intralaminar thalamic nuclei lesions: widespread impact on dopamine denervation-mediated cellular defects in the rat basal ganglia. *J. Neuropathol. Exp. Neurol.*, **63**, 20–31.

Barroso-Chinea, P., Castle, M., Aymerich, M.S., Perez-Manso, M., Erro, E., Tunon, T. & Lanciego, J.L. (2007) Expression of the mRNAs encoding for the vesicular glutamate transporters 1 and 2 in the rat thalamus. *J. Comp. Neurol.*, **501**, 703–715.

Bellocchio, E.E., Reimer, R.J., Fremeau, R.T. Jr & Edwards, R.H. (2000) Uptake of glutamate into synaptic vesicles by an inorganic phosphate transporter. *Science*, **289**, 957–960.

Bennett, B.D. & Bolam, J.P. (1994) Synaptic input and output of parvalbumin-immunoreactive neurons in the neostriatum of the rat. *Neuroscience*, **62**, 707–719.

Berretta, S., Parthasarathy, H.B. & Graybiel, A.M. (1997) Local release of GABAergic inhibition in the motor cortex induces immediate-early gene expression in indirect pathway neurons of the striatum. *J. Neurosci.*, **17**, 4752–4763.

Betarbet, R., Poisik, O., Sherer, T.B. & Greenamyre, J.T. (2004) Differential expression and ser897 phosphorylation of striatal N-methyl-d-aspartate receptor subunit NR1 in animal models of Parkinson's disease. *Exp. Neurol.*, **187**, 76–85.

Blanchet, P.J., Konitsiotis, S. & Chase, T.N. (1998) Amantadine reduces levodopa-induced dyskinesias in parkinsonian monkeys. *Mov. Disord.*, **13**, 798–802.

Blanchet, P.J., Konitsiotis, S., Whittemore, E.R., Zhou, Z.L., Woodward, R.M. & Chase, T.N. (1999) Differing effects of N-methyl-D-aspartate receptor subtype selective antagonists on dyskinesias in levodopa-treated 1-methyl-4-phenyl-tetrahydropyridine monkeys. *J. Pharmacol. Exp. Ther.*, **290**, 1034–1040.

Calabresi, P., Mercuri, N.B., Sancesario, G. & Bernardi, G. (1993) Electrophysiology of dopamine-denervated striatal neurons. Implications for Parkinson's disease. *Brain*, **116**, 433–452.

Calabresi, P., Pisani, A., Centonze, D. & Bernardi, G. (1997) Synaptic plasticity and physiological interactions between dopamine and glutamate in the striatum. *Neurosci. Biobehav. Rev.*, **21**, 519–523.

Calabresi, P., Pisani, A., Mercuri, N.B. & Bernardi, G. (1996) The corticostriatal projection: from synaptic plasticity to dysfunctions of the basal ganglia. *Trends Neurosci.*, **19**, 19–24.

Centonze, D., Gubellini, P., Picconi, B., Calabresi, P., Giacomini, P. & Bernardi, G. (1999) Unilateral dopamine denervation blocks corticostriatal LTP. *J. Neurophysiol.*, **82**, 3575–3579.

Charara, A., Sidibe, M. & Smith, Y. (2002) Basal ganglia circuitry and synaptic connectivity. In: Tarsy, D., Vitek, J.L. & Lozano, A.M. (Eds), *Surgical Treatment of Parkionson's Disease and Other Movement Disorders.* Humana Press Inc., Totowa, NJ, pp. 19–39

Crossman, A.R. (1989) Neural mechanisms in disorders of movement. *Comp. Biochem. Physiol. A*, **93**, 141–149.

Day, M., Wang, Z., Ding, J., An, X., Ingham, C.A., Shering, A.F., Wokosin, D., Ilijic, E., Sun, Z., Sampson, A.R., Mugnaini, E., Deutch, A.Y., Sesack, S.R., Arbuthnott, G.W. & Surmeier, D.J. (2006) Selective elimination of glutamatergic synapses on striatopallidal neurons in Parkinson disease models. *Nat. Neurosci.*, **9**, 251–259.

DeLong, M.R. (1990) Primate models of movement disorders of basal ganglia origin. *Trends Neurosci.*, **13**, 281–285.

Dube, L., Smith, A.D. & Bolam, J.P. (1988) Identification of synaptic terminals of thalamic or cortical origin in contact with distinct medium-size spiny neurons in the rat neostriatum. *J. Comp. Neurol.*, **267**, 455–471.

Eberling, J.L., Bankiewicz, K.S., Pivirotto, P., Bringas, J., Chen, K., Nowotnik, D.P., Steiner, J.P., Budinger, T.F. & Jagust, W.J. (1999) Dopamine transporter loss and clinical changes in MPTP-lesioned primates. *Brain Res.*, **832**, 184–187.

Elsworth, J.D., Brittan, M.S., Taylor, J.R., Sladek, J.R., Jral-Tikriti, M.S., Zea-Ponce, Y., Innis, R.B., Redmond, D.E. & JrRoth, R.H. (1996) Restoration of dopamine transporter density in the striatum of fetal ventral mesencephalon-grafted, but not sham-grafted, MPTP-treated parkinsonian monkeys. *Cell Transplant*, **5**, 315–325.

Fremeau, R.T. Jr, Burman, J., Qureshi, T., Tran, C.H., Proctor, J., Johnson, J., Zhang, H., Sulzer, D., Copenhagen, D.R., Storm-Mathisen, J., Reimer, R.J., Chaudhry, F.A. & Edwards, R.H. (2002) The identification of vesicular glutamate transporter 3 suggests novel modes of signaling by glutamate. *Proc. Natl Acad. Sci. USA*, **99**, 14488–14493.

Fremeau, R.T. Jr, Troyer, M.D., Pahner, I., Nygaard, G.O., Tran, C.H., Reimer, R.J., Bellocchio, E.E., Fortin, D., Storm-Mathisen, J. & Edwards, R.H. (2001) The expression of vesicular glutamate transporters defines two classes of excitatory synapse. *Neuron*, **31**, 247–260.

Fremeau, R.T. Jr, Voglmaier, S., Seal, R.P. & Edwards, R.H. (2004) VGLUTs define subsets of excitatory neurons and suggest novel roles for glutamate. *Trends Neurosci.*, **27**, 98–103.

Fujiyama, F., Unzai, T., Nakamura, K., Nomura, S. & Kaneko, T. (2006) Difference in organization of corticostriatal and thalamostriatal synapses between patch and matrix compartments of rat neostriatum. *Eur. J. Neurosci.*, **24**, 2813–2824.

Gras, C., Herzog, E., Bellenchi, G.C., Bernard, V., Ravassard, P., Pohl, M., Gasnier, B., Giros, B. & Mestikawy, S.E. (2002) A third vesicular glutamate transporter expressed by cholinergic and serotonergic neurons. *J. Neurosci.*, **22**, 5442–5451.

Graybiel, A.M. (1990) Neurotransmitters and neuromodulators in the basal ganglia. *Trends Neurosci.*, **13**, 244–254.

Harkany, T., Hartig, W., Berghuis, P., Dobszay, M.B., Zilberter, Y., Edwards, R.H., Mackie, K. & Ernfors, P. (2003) Complementary distribution of type 1 cannabinoid receptors and vesicular glutamate transporter 3 in basal forebrain suggests input-specific retrograde signalling by cholinergic neurons. *Eur. J. Neurosci.*, **18**, 1979–1992.

Henderson, J.M., Carpenter, K., Cartwright, H. & Halliday, G.M. (2000a) Loss of thalamic intralaminar nuclei in progressive supranuclear palsy and Parkinson's disease: clinical and therapeutic implications. *Brain*, **123**, 1410–1421.

Henderson, J.M., Carpenter, K., Cartwright, H. & Halliday, G.M. (2000b) Degeneration of the centre median-parafascicular complex in Parkinson's disease. *Ann. Neurol.*, **47**, 345–352.

Herzog, E., Bellenchi, G.C., Gras, C., Bernard, V., Ravassard, P., Bedet, C., Gasnier, B., Giros, B. & El Mestikawy, S. (2001) The existence of a second vesicular glutamate transporter specifies subpopulations of glutamatergic neurons. *J. Neurosci.*, **21**, RC181.

Hisano, S., Hoshi, K., Ikeda, Y., Maruyama, D., Kanemoto, M., Ichijo, H., Kojima, I., Takeda, J. & Nogami, H. (2000) Regional expression of a gene encoding a neuron-specific Na(+)-dependent inorganic phosphate cotransporter (DNPI) in the rat forebrain. *Brain Res. Mol. Brain Res.*, **83**, 34–43.

Hisano, S., Sawada, K., Kawano, M., Kanemoto, M., Xiong, G., Mogi, K., Sakata-Haga, H., Takeda, J., Fukui, Y. & Nogami, H. (2002) Expression of inorganic phosphate/vesicular glutamate transporters (BNPI/VGLUT1 and DNPI/VGLUT2) in the cerebellum and precerebellar nuclei of the rat. *Brain Res. Mol. Brain Res.*, **107**, 23–31.

Hur, E.E. & Zaborszky, L. (2005) Vglut2 afferents to the medial prefrontal and primary somatosensory cortices: a combined retrograde tracing in situ hybridization. *J. Comp. Neurol.*, **483**, 351–373.

Ingham, C.A., Hood, S.H., Taggart, P. & Arbuthnott, G.W. (1998) Plasticity of synapses in the rat neostriatum after unilateral lesion of the nigrostriatal dopaminergic pathway. *J. Neurosci.*, **18**, 4732–4743.

Ingham, C.A., Hood, S.H., van Maldegem, B., Weenink, A. & Arbuthnott, G.W. (1993) Morphological changes in the rat neostriatum after unilateral

6-hydroxydopamine injections into the nigrostriatal pathway. *Exp. Brain Res.*, **93**, 17–27.
Kashani, A., Betancur, C., Giros, B., Hirsch, E. & El Mestikauy, S. (2007) Altered expression of vesicular glutamate transporters vGluT2 in Parkinson's disease. *Neurobiol. Aging.*, **28**, 568–578.
Kemp, J.M. & Powell, T.P. (1971) The termination of fibres from the cerebral cortex and thalamus upon dendritic spines in the caudate nucleus: a study with the Golgi method. *Philos. Trans. R. Soc. Lond. B Biol. Sci.*, **262**, 429–439.
Kotter, R. (1994) Postsynaptic integration of glutamatergic and dopaminergic signals in the striatum. *Prog. Neurobiol.*, **44**, 163–196.
Kurlan, R., Kim, M.H. & Gash, D.M. (1991) Oral levodopa dose-response study in MPTP-induced hemiparkinsonian monkeys: Assessment with a new rating scale for monkey parkinsonian. *Mov. Disorders.*, **6**, 111–118.
Lacey, C.J., Boyes, J., Gerlach, O., Chen, L., Magill, P.J. & Bolam, J.P. (2005) GABA (B) receptors at glutamatergic synapses in the rat striatum. *Neuroscience*, **136**, 1083–1095.
Lapper, S.R. & Bolam, J.P. (1992) Input from the frontal cortex and the parafascicular nucleus to cholinergic interneurons in the dorsal striatum of the rat. *Neuroscience*, **51**, 533–545.
Lapper, S.R., Smith, Y., Sadikot, A.F., Parent, A. & Bolam, J.P. (1992) Cortical input to parvalbumin-immunoreactive neurones in the putamen of the squirrel monkey. *Brain Res.*, **580**, 215–224.
Lei, W., Jiao, Y., Del Mar., N. & Reiner, A. (2004) Evidence for differential cortical input to direct pathway versus indirect pathway striatal projection neurons in rats. *J. Neurosci.*, **24**, 8289–8299.
Lindefors, N. & Ungerstedt, U. (1990) Bilateral regulation of glutamate tissue and extracellular levels in caudate-putamen by midbrain dopamine neurons. *Neurosci. Lett.*, **115**, 248–252.
Meshul, C.K., Cogen, J.P., Cheng, H.W., Moore, C., Krentz, L. & McNeill, T.H. (2000) Alterations in rat striatal glutamate synapses following a lesion of the cortico- and/or nigrostriatal pathway. *Exp. Neurol.*, **165**, 191–206.
Miller, G.W., Staley, J.K., Heilman, C.J., Perez, J.T., Mash, D.C., Rye, D.B. & Levey, A.I. (1997) Immunochemical analysis of dopamine transporter protein in Parkinson's disease. *Ann. Neurol.*, **41**, 530–539.
Montana, V., Ni, Y., Sunjara, V., Hua, X. & Parpura, V. (2004) Vesicular glutamate transporter-dependent glutamate release from astrocytes. *J. Neurosci.*, **24**, 2633–2642.
Palfi, S., Leventhal, L., Chu, Y., Ma, S.Y., Emborg, M., Bakay, R., Deglon, N., Hantraye, P., Aebischer, P. & Kordower, J.H. (2002) Lentivirally delivered glial cell line-derived neurotrophic factor increases the number of striatal dopaminergic neurons in primate models of nigrostriatal degeneration. *J. Neurosci.*, **22**, 4942–4954.
Papa, S.M. & Chase, T.N. (1996) Levodopa-induced dyskinesias improved by a glutamate antagonist in Parkinsonian monkeys. *Ann. Neurol.*, **39**, 574–578.
Parent, A. & Hazrati, L.N. (1995) Functional anatomy of the basal ganglia. I. The cortico-basal ganglia-thalamo-cortical loop. *Brain Res. Brain Res. Rev.*, **20**, 91–127.
Parthasarathy, H.B. & Graybiel, A.M. (1997) Cortically driven immediate-early gene expression reflects modular influence of sensorimotor cortex on identified striatal neurons in the squirrel monkey. *J. Neurosci.*, **17**, 2477–2491.
Perez-Otano, I., Oset, C., Luquin, M.R., Herrero, M.T., Obeso, J.A. & Del Rio, J. (1994) MPTP-induced parkinsonism in primates: pattern of striatal dopamine loss following acute and chronic administration. *Neurosci. Lett.*, **175**, 121–125.
Peters, A., Palay, S. & Webster, H.D. (1991) The fine structure of the nervous system: Neurons and their supporting cells. Oxford University Press, New York, p. 494.
Raju, D.V., Shah, D.J., Wright, T.M., Hall, R.A. & Smith, Y. (2006) Differential synaptology of vGluT2-containing thalamostriatal afferents between the patch and matrix compartments in rats. *J. Comp. Neurol.*, **499**, 231–243.
Raju, D.V. & Smith, Y. (2005a) Differential localization of vesicular glutamate transporters 1 and 2 in the rat striatum. In: Bolam, J.P., Ingham, C.A. & Magill, P.J. (Eds), *Basal Ganglia VIII*. Springer Science and Business Media, New York, pp. 601–610
Sadikot, A.F., Parent, A., Smith, Y. & Bolam, J.P. (1992) Efferent connections of the centromedian and parafascicular thalamic nuclei in the squirrel monkey: a light and electron microscopic study of the thalamostriatal projection in relation to striatal heterogeneity. *J. Comp. Neurol.*, **320**, 228–242.
Sidibe, M. & Smith, Y. (1999) Thalamic inputs to striatal interneurons in monkeys: synaptic organization and co-localization of calcium binding proteins. *Neuroscience*, **89**, 1189–1208.
Smith, A.D. & Bolam, J.P. (1990) The neural network of the basal ganglia as revealed by the study of synaptic connections of identified neurones. *Trends Neurosci.*, **13**, 259–265.
Smith, Y., Raju, D.V., Pare, J.F. & Sidibe, M. (2004) The thalamostriatal system: a highly specific network of the basal ganglia circuitry. *Trends Neurosci.*, **27**, 520–527.
Starr, M.S. (1995) Glutamate/dopamine D1/D2 balance in the basal ganglia and its relevance to Parkinson's disease. *Synapse*, **19**, 264–293.
Stephens, B., Mueller, A.J., Shering, A.F., Hood, S.H., Taggart, P., Arbuthnott, G.W., Bell, J.E., Kilford, L., Kingsbury, A.E., Daniel, S.E. & Ingham, C.A. (2005) Evidence of a breakdown of corticostriatal connections in Parkinson's disease. *Neuroscience*, **132**, 741–754.
Takamori, S., Rhee, J.S., Rosenmund, C. & Jahn, R. (2000) Identification of a vesicular glutamate transporter that defines a glutamatergic phenotype in neurons. *Nature*, **407**, 189–194.
Takamori, S., Rhee, J.S., Rosenmund, C. & Jahn, R. (2001) Identification of differentiation-associated brain-specific phosphate transporter as a second vesicular glutamate transporter (VGLUT2). *J. Neurosci.*, **21**, RC182.
Todd, A.J., Hughes, D.I., Polgar, E., Nagy, G.G., Mackie, M., Ottersen, O.P. & Maxwell, D.J. (2003) The expression of vesicular glutamate transporters VGLUT1 and VGLUT2 in neurochemically defined axonal populations in the rat spinal cord with emphasis on the dorsal horn. *Eur. J. Neurosci.*, **17**, 13–27.
Villalba, R.M., Raju, D.V., Hall, R.A. & Smith, Y. (2006a) GABA(B) receptors in the centromedian/parafascicular thalamic nuclear complex: an ultrastructural analysis of GABA(B) R1 and GABA(B) R2 in the monkey thalamus. *J. Comp. Neurol.*, **496**, 269–287.
Villalba, R.M., Verreault, M. & Smith, Y. (2006b) Spine loss in the striatum of MPTP-treated monkeys: a correlation with the degree ofstriatal dopaminergic denervation. *Soc. Neurosci. Abstract*, 431.415.
Wilson, C.J., Chang, H.T. & Kitai, S.T. (1990) Firing patterns and synaptic potentials of identified giant aspiny interneurons in the rat neostriatum. *J. Neurosci.*, **10**, 508–519.
Wilson, N.R., Kang, J., Hueske, E.V., Leung, T., Varoqui, H., Murnick, J.G., Erickson, J.D. & Liu, G. (2005) Presynaptic regulation of quantal size by the vesicular glutamate transporter VGLUT1. *J. Neurosci.*, **25**, 6221–6234.
Wojcik, S.M., Rhee, J.S., Herzog, E., Sigler, A., Jahn, R., Takamori, S., Brose, N. & Rosenmund, C. (2004) An essential role for vesicular glutamate transporter 1 (VGLUT1) in postnatal development and control of quantal size. *Proc. Natl Acad. Sci. USA*, **101**, 7158–7163.